Stoichiometric expression of mtHsp40 and mtHsp70 modulates mitochondrial morphology and cristae structure via $Opa1_L$ cleavage

Byoungchun Lee[a], Younghee Ahn[b], Sung-Myung Kang[a], Youngjin Park[c], You-Jin Jeon[d], Jong M. Rho[b], and Sung-Woo Kim[b]

[a]Southern Alberta Cancer Research Institute, Department of Biochemistry and Molecular Biology, and [b]Department of Pediatrics and Clinical Neurosciences, Alberta Children's Hospital Research Institute for Child and Maternal Health, University of Calgary, Calgary, AB T2N 4N1, Canada; [c]College of Medicine, University of Dong-A, Dong-A Medical Center, Busan 602-714, Republic of Korea; [d]Department of Marine Life Science, Jeju National University, Jeju 690-756, Republic of Korea

ABSTRACT **Deregulation of mitochondrial heat-shock protein 40 (mtHsp40) and dysfunction of mtHsp70 are associated with mitochondrial fragmentation, suggesting that mtHsp40 and mtHsp70 may play roles in modulating mitochondrial morphology. However, the mechanism of mitochondrial fragmentation induced by mtHsp40 deregulation and mtHsp70 dysfunction remains unclear. In addition, the functional link between mitochondrial morphology change upon deregulated mtHsp40/mtHsp70 and mitochondrial function has been unexplored. Our coimmunoprecipitation and protein aggregation analysis showed that both overexpression and depletion of mtHsp40 accumulated aggregated proteins in fragmented mitochondria. Moreover, mtHsp70 loss and expression of a mtHsp70 mutant lacking the client-binding domain caused mitochondrial fragmentation. Together the data suggest that the molecular ratio of mtHsp40 to mtHsp70 is important for their chaperone function and mitochondrial morphology. Whereas mitochondrial translocation of Drp1 was not altered, optic atrophy 1 (Opa1) short isoform accumulated in fragmented mitochondria, suggesting that mitochondrial fragmentation in this study results from aberration of mitochondrial inner membrane fusion. Finally, we found that fragmented mitochondria were defective in cristae development, OXPHOS, and ATP production. Taken together, our data suggest that impaired stoichiometry between mtHsp40 and mtHsp70 promotes $Opa1_L$ cleavage, leading to cristae opening, decreased OXPHOS, and triggering of mitochondrial fragmentation after reduction in their chaperone function.**

Monitoring Editor
Thomas D. Fox
Cornell University

Received: Feb 25, 2014
Revised: Mar 19, 2015
Accepted: Apr 10, 2015

INTRODUCTION

Opposing mitochondrial fusion and fission are key events regulating mitochondrial morphology and play critical roles in maintaining a functional pool of mitochondria (Collins *et al.*, 2002; Cereghetti *et al.*, 2008; Gomes *et al.*, 2011). During promotion of mitochondrial fission, the cytosolic GTPase dynamin-related protein 1 (Drp1) is recruited independently to the mitochondrial outer membrane by an array of integral outer membrane proteins—mitochondrial fission protein 1 (Fis1), mitochondrial fission factor (Mff), and mitochondrial dynamics proteins of 49 and 51 kDa (MiD49 and MiD51; Yoon *et al.*, 2003; Otera *et al.*, 2010; Zhao *et al.*, 2011; Loson *et al.*, 2013). Moreover, mitochondria sense mitochondrial stresses such as membrane depolarization and apoptotic cell death, which shifts mitochondrial morphology to fragmented punctae (Cereghetti *et al.*, 2008; Suen *et al.*, 2008). Mitochondrial fusion depends on two outer membrane–bound GTPases—mitofusin 1 (Mfn1) and mitofusin 2 (Mfn2)—and one inner membrane–bound GTPase, optic atrophy 1 (Opa1;

This article was published online ahead of print in MBoC in Press (http://www.molbiolcell.org/cgi/doi/10.1091/mbc.E14-02-0762) on April 22, 2015.

Address correspondence to: Sung-Woo Kim (swkim@ucalgary.ca).

Abbreviations used: DOX, doxycycline; FCCP, carbonyl cyanide-4-(trifluoromethoxy)phenylhydrazone; MKT-077, 1-ethyl-2-[[3-ethyl-5-(3-methyl-2(3H)-benzothiazolylidene)-4-oxo-2-thiazolidinylidene]methyl]-pyridinium chloride; NP40, Nonidet P-40; RNAi, RNA interference; ROT, rotenone.

© 2015 Lee *et al.* This article is distributed by The American Society for Cell Biology under license from the author(s). Two months after publication it is available to the public under an Attribution–Noncommercial–Share Alike 3.0 Unported Creative Commons License (http://creativecommons.org/licenses/by-nc-sa/3.0).

"ASCB®," "The American Society for Cell Biology®," and "Molecular Biology of the Cell®" are registered trademarks of The American Society for Cell Biology.

Chen *et al.*, 2003; Cipolat *et al.*, 2004). Of interest, Opa1 has several isotypes that are soluble in the intermembrane space or bound to inner membrane and coordinate cristae junctions, promoting cristae density and inner membrane fusion (Frezza *et al.*, 2006; Loson *et al.*, 2013). It has been reported that genetic depletion of Mfn1/2 and accumulation of Opa1 short isoform ($Opa1_S$) after the cleavage of $Opa1_L$ promote mitochondrial fragmentation (Guillery *et al.*, 2008; Gegg *et al.*, 2010).

The mitochondrial heat-shock proteins mtHsp40 and mtHsp70 are classified in the Hsp40 and Hsp70 families, respectively. Mechanistically, mtHsp40 and mtHsp70 cooperate to maintain mitochondrial proteostasis by supporting protein (re)folding (Hartl *et al.*, 2011). Both client-bound and free forms of mtHsp40 interact with the ATPase domain of mtHsp70 (Kampinga and Craig, 2010). In vitro findings demonstrated that elevated mtHsp40 protein without concomitant increase of mtHsp70 protein inhibited mtHsp70 activity of protein deaggregation (Hageman *et al.*, 2011; Iosefson *et al.*, 2012), indicating that the stoichiometry of mtHsp40–mtHsp70 is critical for their chaperone activity. Both $mtHsp40_L$ and $mtHsp40_S$, two splice variants of mtHsp40, bind mtHsp70 to mediate (re)folding of nascent polypeptides in vitro and in vivo (Ahn *et al.*, 2010; Iosefson *et al.*, 2012), and overexpression of both forms promotes apoptosis (Kim *et al.*, 2004). One study showed that loss-of-function mutation of mtHsp70 in Parkinson disease patients increased mitochondrial protein instability, leading to mitochondrial fragmentation (Burbulla *et al.*, 2010). In addition, our recent study showed that deregulation of mtHsp40 resulted in mitochondrial fragmentation in a way that depended on Drp1 (Lee *et al.*, 2012), suggesting that mtHsp40 may play important roles together with mtHsp70 in modulating mitochondrial morphology. However, little is known about the link between mitochondrial morphology and the chaperone function of mtHsp40–mtHsp70. Although it has been proposed that Drp1 is required for mitochondrial fragmentation, it is unclear how the deregulated ratio of mtHsp40–mtHsp70 affects mitochondrial morphology. Finally, the relationship between mitochondrial morphology and function has been unexplored. We therefore set out to investigate how mitochondria become fragmented and which mitochondrial function is altered by finely altering the ratio of mtHsp40–mtHsp70. Our results show that the molecular ratio of mtHsp40–mtHsp70 determines mitochondrial morphology, cristae formation, and oxidative phosphorylation (OXPHOS) activity via $Opa1_L$ cleavage.

RESULTS

Mitochondrial morphology reversibly changes according to mtHsp40 levels

Given that both overexpression and knockdown of mtHsp40 cause mitochondrial fragmentation (Lee *et al.*, 2012), we sought to confirm whether the level of mtHsp40 is a determinant of mitochondrial morphology by using 293-mitoRFP-$mtHsp40_L$ cells stably expressing mitochondrion-targeted DsRed2 (mitoRFP) and inducibly expressing $mtHsp40_L$ with doxycycline (DOX). This cell line highly induced $mtHsp40_L$ in the presence of 100 ng/ml DOX (Figure 1A). Consistent with our previous studies (Lee *et al.*, 2012), most mitochondria of cells overexpressing $mtHsp40_L$ became fragmented, whereas control mitochondria developed well the filamentous network (Figure 1B). We used a morphology-scoring assay in which each cell was categorized as having long tubules (tubular) or short puncta of mitochondria (fragmented). DOX induction of $mtHsp40_L$ shifted mitochondrial morphology from tubules to punctae in >70% of cells (Figure 1C). To determine whether there is a threshold of $mtHsp40_L$ level for triggering mitochondrial fragmentation, we treated 293-mitoRFP-$mtHsp40_L$ cells with a gradient concentration (0–100 ng/ml) of DOX. DOX at 5 ng/ml induced $mtHsp40_L$ 33-fold higher than control, and ~80% of cells had severely fragmented mitochondria (Figure 1, D and E). DOX doses >5 ng/ml had no additional effect on mitochondrial morphology.

Mitochondrial fragmentation is reversibly induced in a response to various stresses such as loss of membrane potential (Legros *et al.*, 2002; Jendrach *et al.*, 2008). Thus we tested whether mitochondrial morphology change here is also reversible according to mtHsp40 level. Of interest, most mitochondria reverted to tubules (Figure 1G and Supplemental Figure S1) after $mtHsp40_L$ levels returned to control level (Figure 1F). These data suggest that the aberrant levels of mtHsp40 reversibly caused mitochondrial fragmentation.

mtHsp70 client-binding activity is decreased in mtHsp40-overexpressing cells

Both isoforms of mtHsp40—$mtHsp40_L$ and $mtHsp40_S$—physically interact with mtHsp70 to promote mitochondrial protein stability (Ahn *et al.*, 2010; Iosefson *et al.*, 2012). To test the effect of $mtHsp40_L$ expression on mtHsp70 interaction with endogenous $mtHsp40_S$, we isolated mitochondria from control and $mtHsp40_L$-overexpressing cells, followed by coimmunoprecipitation using anti-mtHsp70 antibodies. We found that the level of $mtHsp40_S$ pulled down by anti-mtHsp70 antibodies in $mtHsp40_L$-overexpressing cells was substantially lower than in control (Figure 2A), suggesting that mtHsp70 interaction with endogenous $mtHsp40_S$ was inhibited in fragmented mitochondria after ectopic expression of $mtHsp40_L$. To confirm this observation, we repeated this experiment from cells treated with a range of DOX concentrations. We found that mtHsp70 interaction with endogenous $mtHsp40_S$ was negatively affected with ≥5 ng/ml DOX (Figure 2B). Given that mtHsp70 requires mtHsp40 in order to bind client proteins (Kampinga and Craig, 2010), we thus proposed that mtHsp40 higher than a threshold can inhibit mtHsp70 interaction with client proteins, leading to reduction of protein (re)folding. To test this hypothesis, we performed a protein aggregation assay. Consistent with previous in vitro experiments (Iosefson *et al.*, 2012), overexpression of $mtHsp40_L$ showed the tendency of elevated protein aggregation in fragmented mitochondria in the presence of NP-40 detergent (Figure 2C). Taken together, these data suggest that overexpression of mtHsp40 inhibits the chaperone function of mtHsp70, leading to fragmented mitochondria.

mtHsp70 activity is critical for maintaining mitochondrial morphology

One study reported that mtHsp70 dysfunction resulted in defects in mitochondrial protein stability and changes in mitochondrial morphology from Parkinson disease patients (Burbulla *et al.*, 2010). To confirm this finding, we used short interfering RNA (siRNA) to knock down mtHsp70. Loss of mtHsp70 caused severe mitochondrial fragmentation in most cells (Figure 3, B and C). In addition, we also tested the effects of the mtHsp70 small inhibitor MKT-077 on mitochondrial morphology. MKT-077 also caused mitochondrial fragmentation in ~60% of cells (Figure 3, E and F). However, MKT-077 did not affect the level of mtHsp40 or mtHsp70 protein levels (Figure 3D). These data indicate that mtHsp70 activity is important for maintaining mitochondrial morphology.

To determine important domain(s) of mtHsp70 in maintaining mitochondrial morphology, we generated C-terminal Flag-tagged mtHsp70 wild type and mutants lacking domains as shown in Figure 4C: full-length mtHsp70 (1–679), mtHsp70 (ΔMTS) lacking mitochondrion-targeting sequence (MTS), mtHsp70 (ΔATPase) lacking the ATPase domain, and mtHsp70 (1–434) lacking the client-binding domain (CBD). We first examined the effect of mtHsp70 overexpression

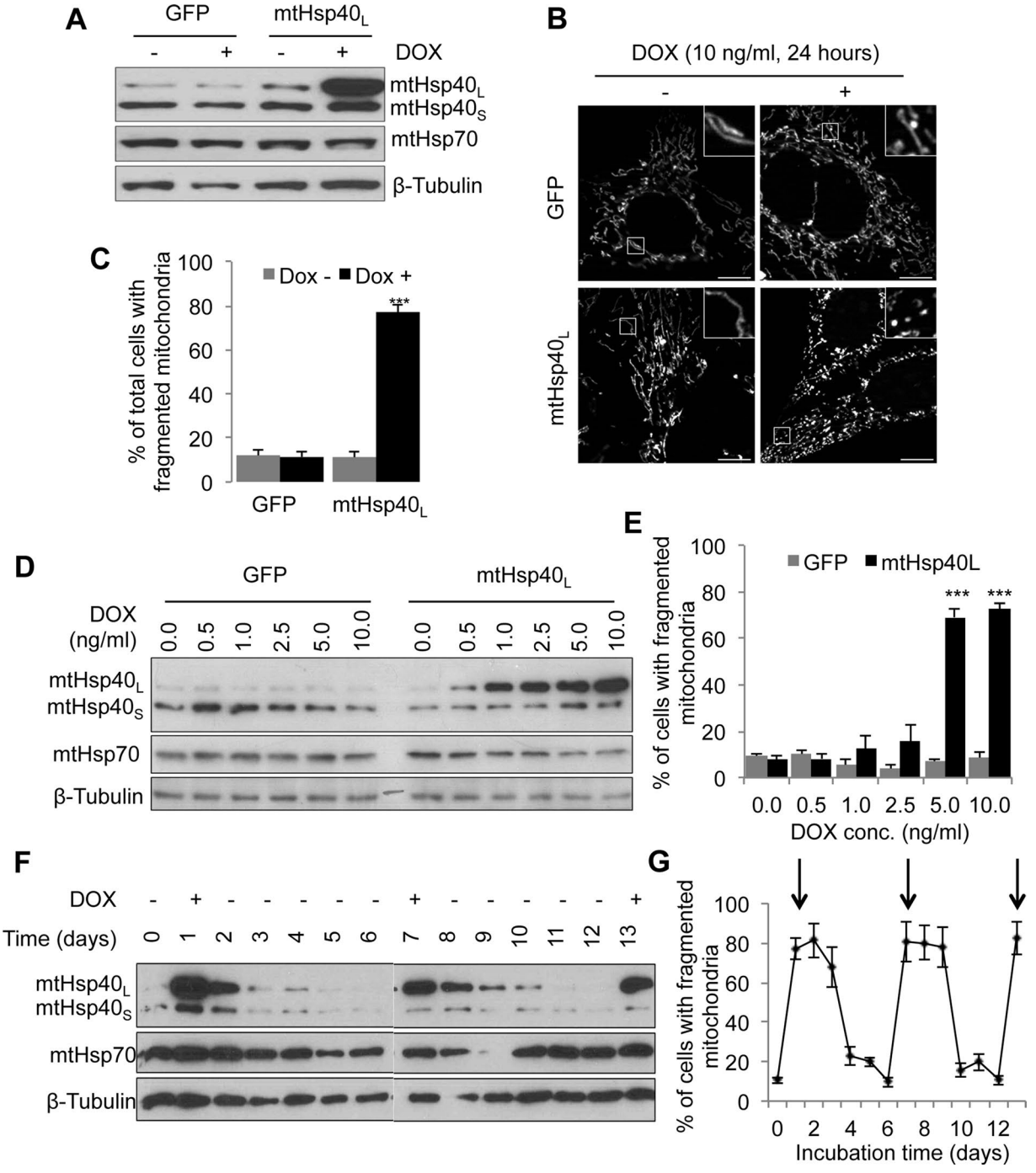

FIGURE 1: Reversible mitochondrial fragmentation corresponding to mtHsp40 levels. (A) DOX induction of mtHsp40$_L$. HEK293-mitoRFP-GFP and -mtHsp40$_L$ cells were treated with PBS or DOX (100 ng/ml for 24 h). Total lysates were analyzed by Western blots using the indicated antibodies. (B) Mitochondrial morphology in cells treated as described in A. Mitochondria were visualized by red fluorescent protein (RFP) fluorescence. Insets, magnified images of boxed regions. Scale bar, 10 μm. (C) Scoring of mitochondrial morphologies for the cells described in B. Each cell was scored into filamentous network (normal) or short puncta (fragmented), and the ratio of cells showing fragmented mitochondria is plotted as percentage of total cells from >200 cells. Data were obtained from three independent experiments. Error bars, SEM; ***$p < 0.001$. (D) Correlated induction of mtHsp40$_L$ with DOX concentration. Scoring of mitochondrial morphologies for the cells as described in C. Cells were treated with indicated amounts of DOX for 24 h, and total lysates were analyzed by Western blotting. (E) Threshold of mtHsp40$_L$ triggering mitochondrial fragmentation. Data were obtained from three independent experiments. Error bars, SEM; ***$p < 0.001$. (F) mtHsp40$_L$ pulse with DOX treatment. HEK293-mitoRFP-mtHsp40$_L$ cells were repetitively incubated with DOX (10 ng/ml for 12 h), washed with PBS, and then cultured for the indicated time. Total lysates were analyzed by Western blotting. (G) Reversible mitochondrial morphology change corresponding to mtHsp40$_L$ levels. Scoring of mitochondrial morphologies for the cells treated as in F. The percentage of cells showing mitochondrial fragmentation is plotted. Arrows indicate DOX treatment. Representative data were obtained from three independent experiments. Error bars, SEM.

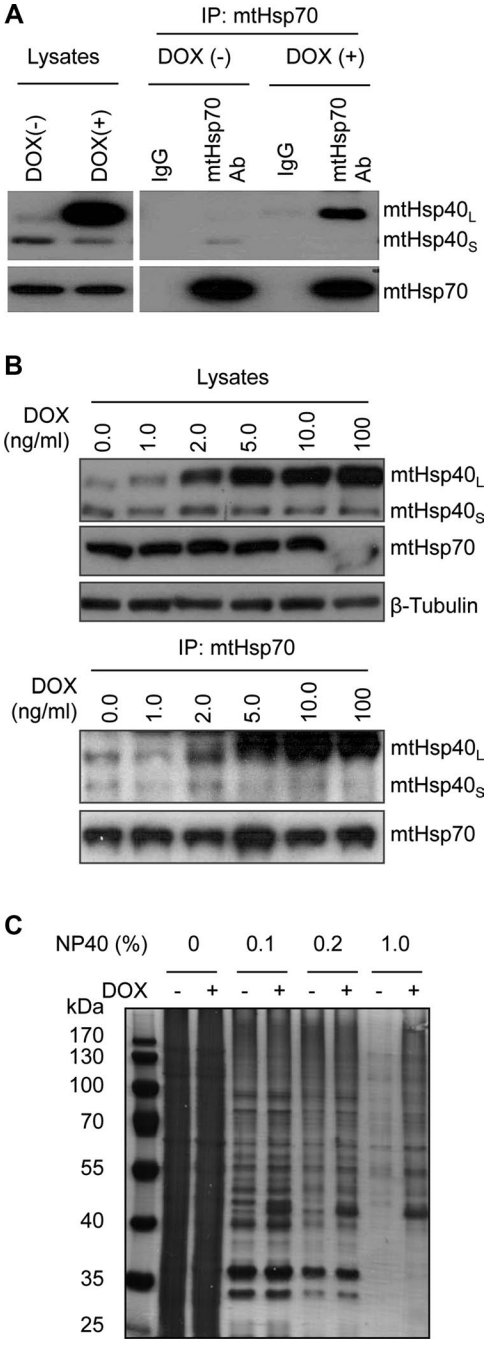

FIGURE 2: Chaperone activity of mtHsp70 is inhibited in fragmented mitochondria of mtHsp40$_L$-overexpressing cells. (A) Decreased mtHsp70 interaction with endogenous mtHsp40$_S$ in mtHsp40$_L$-overexpressing mitochondria. Left, lysates from HEK293-mitoRFP-mtHsp40$_L$ cells in the absence (control) or presence of DOX analyzed by Western blotting for mtHsp40 and mtHsp70. Right, mtHsp70 immunoprecipitated using anti-mtHsp70 antibodies, with endogenous mtHsp40$_S$ detected with anti-mtHsp40 antibodies. mtHsp70 was included as a loading control. (B) Threshold of ectopic mtHsp40$_L$ inhibiting mtHsp70 interaction with endogenous mtHsp40$_S$. Left, lysates from HEK293-mitoRFP-mtHsp40$_L$ cells with indicated amount of DOX analyzed by Western blotting for mtHsp40 and mtHsp70. Right, mtHsp70 immunoprecipitated from the foregoing lysates and endogenous mtHsp40$_S$ detected with anti-mtHsp40 antibodies. mtHsp70 was included as a loading control. (C) Increased aggregated proteins in fragmented mitochondria of mtHsp40$_L$-overexpressing cells. Detergent (NP40)-insoluble mitochondrial proteins from control or mtHsp40$_L$-overexpressing mitochondria visualized by silver staining.

on mitochondrial morphology by introducing a range (0–1 μg) of mtHsp70-Flag into HeLa-mitoRFP cells. Consistent with a previous finding (Burbulla *et al.*, 2010), mitochondrial morphology was not affected by overexpression of mtHsp70 (Figure 4, A and B). Wild-type and mutant mtHsp70s were highly expressed, and all forms of mtHsp70 harboring MTS produced both unprocessed and processed forms of mtHsp70 (Figure 4D). Immunostaining results revealed that all forms of mtHsp70 harboring MTS colocalized well with mitoRFP, indicating their localization to mitochondria, whereas mtHsp70 (ΔMTS) primarily localized in the cytosol (Figure 4E). Although sole deletion of either MTS or ATPase domain had no significant effect on mitochondrial morphology, the ectopic expression of mtHsp70 (1–434) resulted in mitochondrial fragmentation in up to 40% of Flag-positive cells (Figure 4, E and F). In addition, a mutant lacking both MTS and CBD did not affect mitochondrial morphology (unpublished data). Collectively these data show that reduction in mtHsp70 activity by depleting mtHsp70 or expressing an mtHsp70 mutant lacking CBD induces mitochondrial fragmentation.

A stoichiometric balance of mtHsp40-mtHsp70 determines mitochondrial morphology

To determine whether concomitant levels of mtHsp70 with mtHsp40 overexpression rescue mitochondrial morphology, we cotransfected HeLa-mitoRFP cells with a combination of full-length mtHsp70 and a range of mtHsp40-Flag (1–500 ng). Ectopic expression of mtHsp40$_L$-Flag was detectable at ≥15 ng plasmid DNA from both control and mtHsp70-transfected cells (Figure 5A). Whereas mitochondria were severely fragmented in most cells at ≥15 ng mtHsp40$_L$-Flag in the absence of mtHsp70 expression, mitochondrial fragmentation was detected at ≥60 ng mtHsp40$_L$-Flag, and the extent of mitochondrial fragmentation was less in mtHsp70-overexpressing cells (Figure 5B). To confirm this observation, we repeated this experiment with one concentration of mtHsp70 (500 ng) and mtHsp40-Flag (50 ng; Figure 5C). Whereas mtHsp40 overexpression alone triggered mitochondrial fragmentation in ~40% of total cells, the concomitant increase of mtHsp40 and mtHsp70 restored tubular morphology (Figure 5, D and E). We also found that individual knockdown of mtHsp40 or mtHsp70 and knockdown of both resulted in severely fragmented mitochondria (Supplemental Figure S2). Together these data suggested that the molecular balance between mtHsp70 and mtHsp40 is important to maintaining mitochondrial morphology.

Opa1$_L$ cleavage is enhanced by imbalance between mtHsp40 and mtHsp70

Causes of mitochondrial fragmentation include promotion of mitochondrial fission by recruiting cytosolic Drp1 to mitochondria and reduction of mitochondrial fusion by reducing Mfn1/2 level or inducing Opa1$_L$ cleavage (Cipolat *et al.*, 2004; Cereghetti *et al.*, 2008; Gegg *et al.*, 2010). Our previous finding showed that knockdown of Drp1 alleviated the effect of mtHsp40 overexpression on mitochondrial fragmentation (Lee *et al.*, 2012). However, the molecular mechanisms remain unclear. To address how mitochondria become fragmented by imbalance of mtHsp40-mtHsp70, we therefore assessed the protein levels of fusion and fission effectors. Immunoblotting analysis revealed that either mtHsp40 overexpression or knockdown did not affect the protein levels of Drp1, Mfn1/2, or Opa1 (Figure 6A). Of interest, whereas the Opa1$_L$ level was reduced, Opa1$_S$ accumulated after both overexpression and knockdown of mtHsp40 compared with control (Figure 6A). The ratio of Opa1$_L$:Opa1$_S$ was greater than threefold lower than control in both mtHsp40$_L$ expression and mtHsp40 knockdown, indicating that Opa1$_L$ cleavage was promoted by mtHsp40 deregulation. A lower ratio of

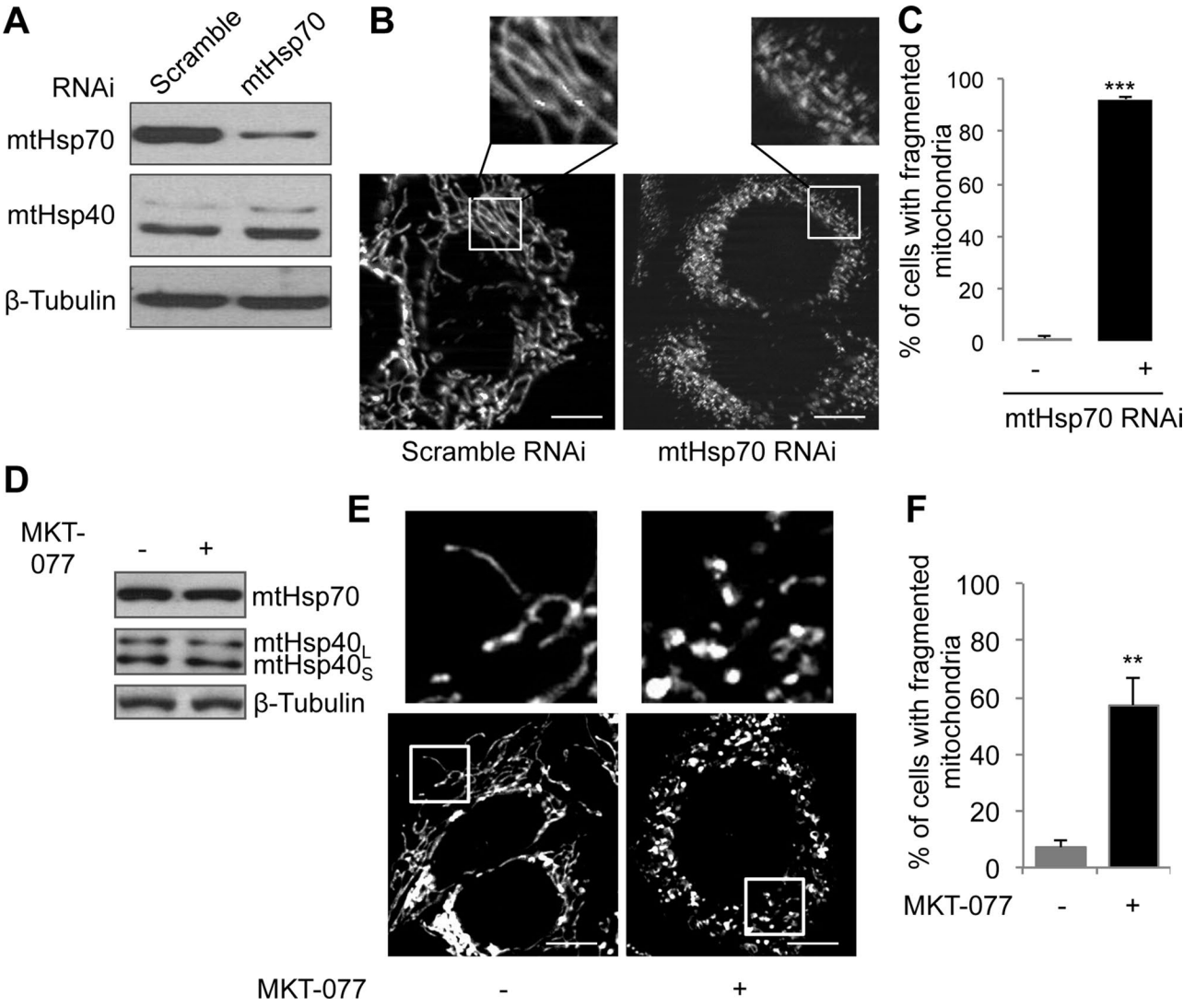

FIGURE 3: Inhibition of mtHsp70 causes mitochondrial fragmentation. (A) Western blot of cell lysates of control (scramble siRNA) and mtHsp70 knockdown (mtHsp70 siRNA) in HeLa-mitoRFP cells. (B) Mitochondrial morphology in HeLa-mitoRFP cells transfected with control siRNA or mtHsp70 siRNA. Also shown are magnified images of boxed regions. Scale bars, 10 μm. (C) Scoring of mitochondrial morphologies for mtHsp70-knockdown experiments. Data were obtained from three independent experiments, with >200 cells scored per experiment. Error bars, SEM; ***$p < 0.001$. (D) Western blot of cell lysates of HeLa-mitoRFP cells treated with control (dimethyl sulfoxide) and MKT-077, a small inhibitor of mtHsp70, using indicated antibodies. (E) Mitochondrial morphology in cells treated with control and MKT-077. Insets, magnified images of boxed regions. Scale bars, 10 μm. (F) Scoring of mitochondrial morphology for MKT-077 treatment. Data were obtained from three independent experiments, with 100 cells scored per experiment. Error bars, SEM; **$p < 0.01$.

$Opa1_L$:$Opa1_S$ was also observed in other cell lines, such as Hs68 and SK-N-SH cells overexpressing $mtHsp40_L$: the ratio of $Opa1_L$:$Opa1_S$ decreased eightfold in Hs68 cells and sevenfold in SK-N-SH cells compared with control (Supplemental Figure S3). Given that expression of two isoforms (isoforms 1 and 7) of Opa1 lacking cleavage site S1 or S2 restores tubular mitochondria (Song *et al.*, 2007), we tested whether the expression of Opa1 isoform 1 ($Opa1_L$-1) lacking S1 can restore mitochondrial tubulation in the presence of $mtHsp40_L$ expression. We observed that $mtHsp40_L$ expression promoted primarily cleavage of Opa1 isoform 7 ($Opa1_L$-7; Figure 6B), and that expression of $Opa1_L$-1(ΔS1) did not restore tubular mitochondria (Figure 6C). Given our previous finding that Drp1 depletion reduced the effect of mtHsp40 overexpression on mitochondrial morphology, we measured the effect of Drp1 depletion on the ratio of $Opa1_L$:$Opa1_S$ and observed that Drp1 depletion did not alter the tendency toward a reduced ratio of $Opa1_L$:$Opa1_S$ upon mtHsp40 overexpression (Supplemental Figure S4).

To address whether the imbalance of mtHsp40-mtHsp70 promoted fission events, we measured Drp1 translocation to mitochondria by immunostaining and mitochondrial fraction analysis. We chose Mff as a positive control because it was reported that Mff expression promoted Drp1 translocation to mitochondria (Otera *et al.*, 2010). Whereas Mff overexpression enhanced Drp1 localization to mitochondria and resulted in mitochondrial fragmentation, $mtHsp40_L$ overexpression caused mitochondrial fragmentation without enhanced Drp1 translocation to mitochondria

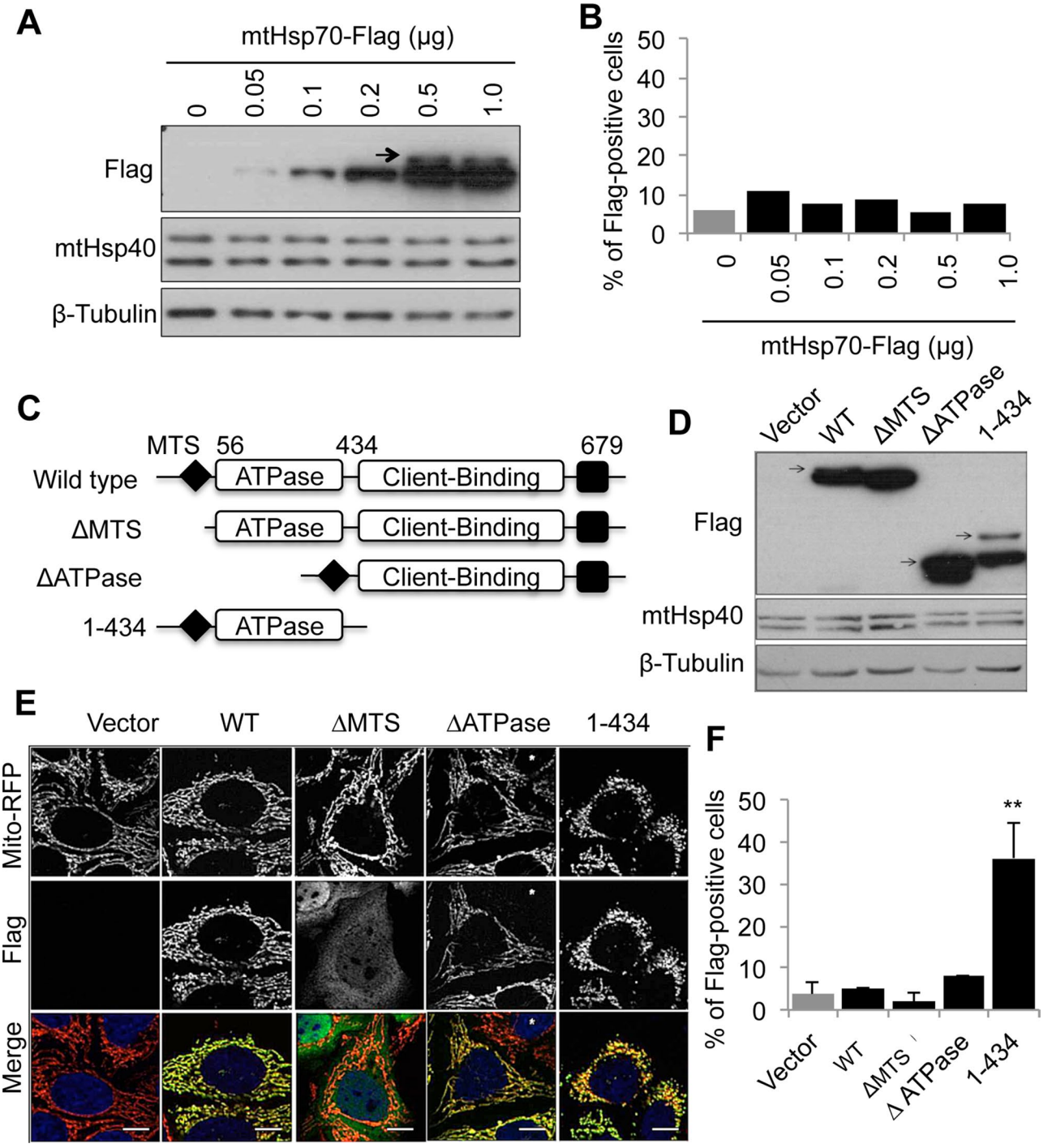

FIGURE 4: Important domains of mtHsp70 for maintaining mitochondrial morphology. (A) Correlated mtHsp70 levels with plasmid amount. Western blot of lysates of HeLa-mitoRFP cells transfected with indicated amount of C-terminal Flag-tagged mtHsp70. (B) Scoring of mitochondrial fragmentation with mtHsp70 overexpression. Cells with fragmented mitochondria as shown in Figure 3B were plotted as the percentage of total cells; $n = 1$. (C) Schematic representation of mtHsp70 constructs used in this study. All constructs were tagged with FLAG at the C-terminus. ATPase, ATPase domain; CBD, client-binding domain; MTS, mitochondrial targeting sequence. (D) Expression of mtHsp70 constructs. Lysates of HeLa-mitoRFP cells transiently expressing mtHsp70 mutants as indicated were analyzed by Western blotting for FLAG, mtHsp40, and β-tubulin (loading control). (E) Representative images of cells transiently transfected by indicated mtHsp70 constructs. Cells were analyzed for mtHsp70-FLAG expression (anti-FLAG) and mitochondrial morphology (RFP). Scale bars, 10 μm. Asterisk denotes untransfected cells. (F) Quantitation of cells showing mitochondrial fragmentation. Scoring and quantitation as described in B. Data were obtained from three independent experiments, with 100 cells scored per experiment. Error bars, SEM; $^{**}p < 0.01$.

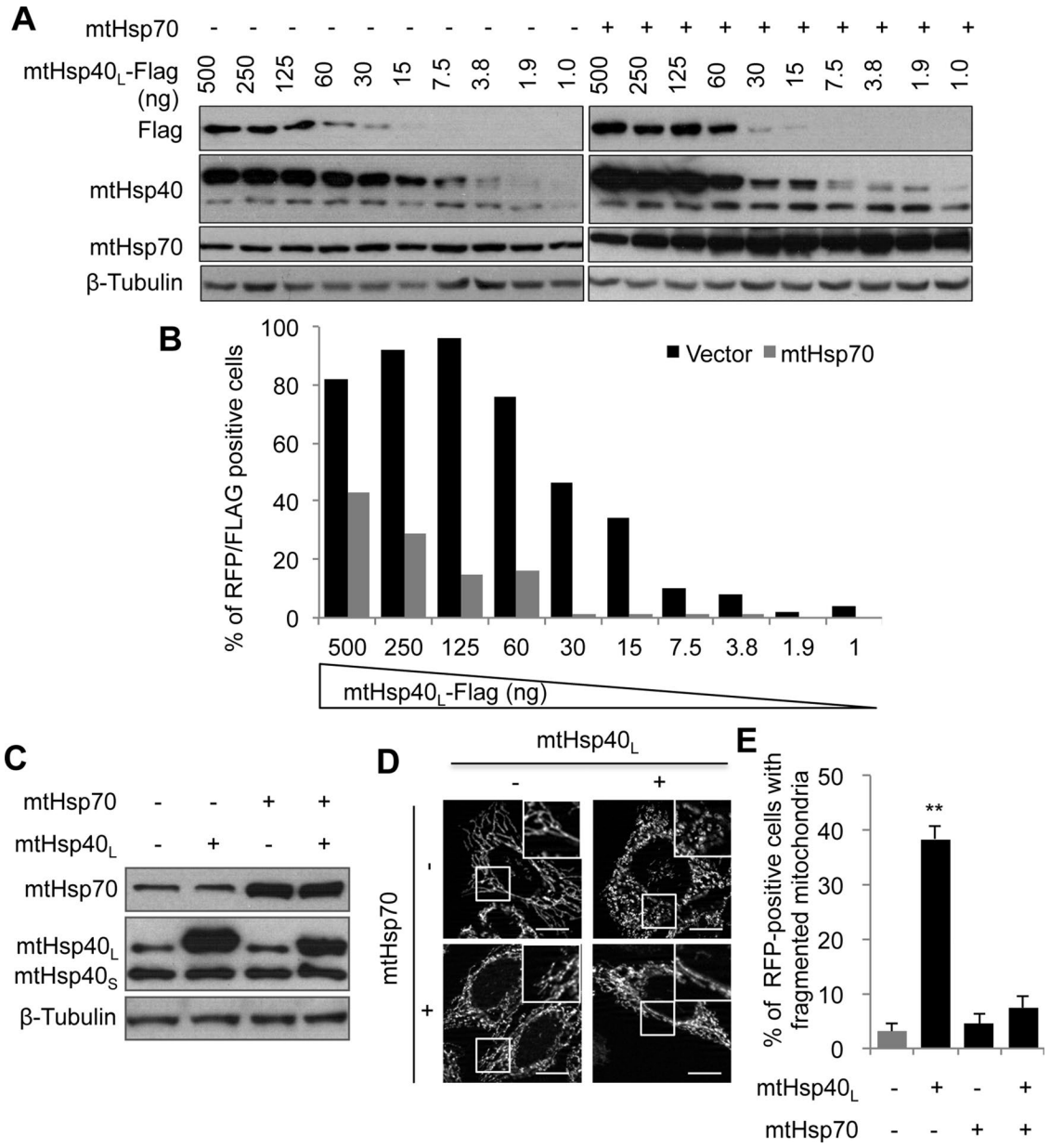

FIGURE 5: Cooperative effect of mtHsp40-mtHsp70 on mitochondrial morphology. (A) Concomitant expression of mtHsp40$_L$ with mtHsp70. HeLa-mitoRFP cells was transiently introduced with a serial amount of mtHsp40$_L$-Flag in the presence of empty vector (control, left) and mtHsp70 (right). Lysates were analyzed by Western blotting for FLAG, mtHsp40, mtHsp70, and β-tubulin (loading control). (B) Quantitation of the percentage of Flag/RFP-positive cells showing fragmented mitochondria; 100 cells; $n = 1$. (C) Coexpression of mtHsp40 and mtHsp70. HeLa-mitoRFP cells were transiently introduced with mtHsp40$_L$ together with empty vector (control) and mtHsp70. Lysates were analyzed by Western blotting for mtHsp40, mtHsp70, and β-tubulin (loading control). (D) Coexpression of mtHsp70 with mtHsp40 restores tubular mitochondria. Mitochondria of cells in C were visualized with RFP. Insets, magnified images of boxed regions. Scale bars, 10 μm. (E) Quantitation of cells with fragmented mitochondria. Data were obtained from three independent experiments, with <100 cells scored per experiment. Error bars, SEM; $^{**}p < 0.01$.

(Figure 6D). In addition, mitochondrial fraction analysis showed no significant increase of mitochondrial Drp1 or hemagglutinin (HA)-Drp1 in the presence of mtHsp40$_L$ expression (Figure 6E). Finally, we also tested whether enhanced outer membrane fusion by expressing Mfn1/2 can suppress mitochondrial fragmentation caused by mtHsp40 expression. Expression of Mfn1-Myc or Mfn2-Myc did not suppress either mitochondrial fragmentation or Opa1$_L$ cleavage (Supplemental Figure S5). Collectively, these observations demonstrate that imbalance of mtHsp40-mtHsp70 inhibits inner membrane fusion through Opa1$_L$-7 cleavage without affecting Drp1 translocation, leading to mitochondrial fragmentation.

Fragmented mitochondria are defective in cristae development, resulting in reduced ATP production and oxygen consumption

To explore the effects of mitochondrial fragmentation on mitochondrial function, we first examined mitochondrial ultrastructure

using transmission electron microscopy (TEM). It was reported that Opa1 mediates cristae formation and inner membrane fusion by enhancing inner membrane junctions (Frezza *et al.*, 2006). Thus we sought to determine whether $Opa1_L$ cleavage caused by mtHsp40 overexpression or knockdown affects inner membrane structure. TEM data showed that fragmented mitochondria in both $mtHsp40_L$-overexpressing and $mtHsp40_L$-deficient cells were defective in cristae structure (Figure 7A). These findings were confirmed in multiple cell lines, including Hs68, SK-N-SH, and HEK293 (Supplemental Figure S6). In contrast, the overall ER structure was not altered. Both $mtHsp40_L$-overexpressing and $mtHsp40_L$-deficient cells showed decreases in ATP level when grown in high-glucose medium (Figure 7D) and galactose medium (Supplemental Figure S7A). In addition, oxygen consumption rate (OCR) was measured to investigate mitochondrial OXPHOS function using a Seahorse Bioscience XF analyzer. The basal OCR in $mtHsp40_L$-overexpressing cells decreased up to ~40% of control, and the basal OCR in mtHsp40-deficient cells was ~70% of control (Figure 7, B and C, and Supplemental Figure S7B). However, OCR in both $mtHsp40_L$-overexpressing and $mtHsp40_L$-deficient cells responded to inhibitors of respiratory chain complexes, indicating that overall OXPHOS activity was reduced in fragmented mitochondria, leading to lower ATP production, but the individual complex of OXPHOS was still functional (Figure 7, B and C, and Supplemental Figure S7B). To test the effects of mitochondrial fragmentation on mitochondrial biogenesis, we quantified mitochondrial DNA (mtDNA) and MitoTracker staining. The data showed that mtDNA and mitochondrial quantity did not change in $mtHsp40_L$-overexpressing or $mtHsp40_L$-deficient cells (Figure 7E and Supplemental Figure S8). Taken together, these results suggest that mtHsp40 deregulation results in cristae remodeling, leading to reduction of ATP production and OXPHOS activity with no effects on mitochondrial DNA replication or mitochondrial biogenesis.

DISCUSSION

Our work elucidates the mechanistic and functional link between the mtHsp40-mtHsp70 complex and mitochondrial morphology. In addition to analysis of mtHsp40 levels, experiments expressing mtHsp70 mutants lacking important domains showed that the molecular balance between mtHsp40 and mtHsp70 is critical for their chaperone function and mitochondrial morphology. Consistently with in vitro findings (Iosefson *et al.*, 2012), our data demonstrate that in vivo stoichiometry of mtHsp40-mtHsp70 is important in maintaining mitochondrial morphology, as well as protein homeostasis. We speculate that an excessive amount of free mtHsp40 inhibits mtHsp70 from binding to substrate proteins, leading to accumulation of misfolded/unfolded proteins. To further reveal the physiological stoichiometry between mtHsp40 and mtHsp70 in vivo, biochemical studies such as mass spectrometry are needed. Given that the mitochondrial unfolded protein response (UPR^{mt}) is stimulated in response to accumulation of unfolded proteins in mitochondria (Pellegrino *et al.*, 2014), it is also necessary to elucidate the effects of imbalance between mtHsp40 and mtHsp70 on UPR^{mt}.

Previous studies showed that mtHsp70 mediates not only mitochondrial protein (re)folding but also protein import (Schmidt *et al.*, 2010). We found that mitochondrial proteins such as mitoRFP (inner membrane), cytochrome *c* (intermembrane space), and Tom20 (outer membrane) primarily localized to fragmented mitochondria in the presence of $mtHsp40_L$ expression (unpublished data), showing that the imbalance of mtHsp40-mtHsp70 inhibits primarily the chaperone function of mtHsp70, but does not affect protein import. To demonstrate this notion more clearly, in vitro mitochondrial protein import assays would of considerable interest.

This work suggests that for the $Opa1_L$ isoform $Opa1_L$-7, cleavage triggered by imbalance between mtHsp40 and mtHsp70 primarily results in mitochondrial fragmentation, which is puzzling, given our previous finding that mitochondrial fragmentation is Drp1 dependent (Lee *et al.*, 2012). In this regard, we hypothesize that inhibition of inner membrane fusion resulting from $Opa1_L$-7 cleavage may stimulate the fission activity of mitochondrial Drp1, leading to mitochondrial fragmentation. To test this hypothesis, one needs to elucidate whether the cleavage of $Opa1_L$-7 is critical for mitochondrial fragmentation by using $Opa1_L$-7 mutant lacking cleavage site S1 or S2. In addition, it is also necessary to test whether Drp1 mutants lacking GTPase activity rescue mitochondrial fragmentation caused by $Opa1_L$-7 cleavage. Furthermore, mechanism(s) by which $Opa1_L$-7 is converted to $Opa1_S$ in the presence of imbalance of mtHsp40-mtHsp70 remain unexplored. Given that several mitochondrial peptidases, including Yme1L (S1 site) and Oma1 (S2 site), differentially cleave $Opa1_L$-7 (Song *et al.*, 2007; Ehses *et al.*, 2009; Head *et al.*, 2009; Anand *et al.*, 2014), one needs to investigate whether the activities of Oma1 and Yme1L are affected by imbalance between mtHsp40 and mtHsp70. Finally, a recent study revealed that ROMO1 is a critical regulator of Opa1 oligomerization (Norton *et al.*, 2014). Therefore it is worth testing whether imbalance of mtHsp40-mtHsp70 affects ROMO1 level and function.

Finally, we find that cristae structure is severely remodeled in fragmented mitochondria, which seems to be coupled with $Opa1_L$ cleavage under an imbalance of mtHsp40-mtHsp70. In addition, we also show that fragmented mitochondria are defective in ATP production and OXPHOS but do not have a significant effect on apoptosis (Lee *et al.*, 2012). One study demonstrated that mitochondrial cristae shape determines respiratory supercomplex assembly in the inner membrane (Cogliati *et al.*, 2013). Thus future studies will explore the link between respiratory supercomplex assembly and imbalance of mtHsp40-mtHsp70.

MATERIALS AND METHODS

Molecular biology

Mitochondrion-targeted DsRed2 (mtRFP) was previously described (Lee *et al.*, 2012). Validated siRNAs (mtHsp40; Mm_Dnaja3_3 FlexiTube siRNA, mtHsp70; Hs_HSPA9_5 FlexiTube siRNA, Drp1; Hs_DNM1L_5 FlexiTube siRNA, and Scramble; FlexiTube Control siRNA) were purchased from Qiagen (Toronto, Canada). HA-Drp1 and Mff-Flag were kind gifts from Hidenori Otera (Kyushu University, Fukuoka, Japan). mtHsp70-Flag mutants were prepared from wild type purchased from OriGene (Rockville, MD). To generate mtHsp70-Flag mutants, PCR was performed using the following primer sequences: full length 1–679 (forward [FW]: 5′-*Bam*HI ATG ATA AGT GCC AGC CGA GCT-3′; reverse [RV]: 5′-*Hin*dIII TTA GAG GTC TTC TTC TGA GAT GAG CTT CTG CTC CTG TTT TTC CTC CTT TTG AT-C TTC C-3′), ΔMTS 57-679 (FW: 5′-*Bam*HI ATG ATA AGT GCC AGC CGA GCT-3′; RV: 5′-*Hin*dIII TTA GAG GTC TTC TTC TGA GAT GAG CTT CTG CTC CTG TTT TTC CTC CTT TTG ATC TTC C-3′), ΔATPase (FW1: 5′-*Bam*HI ATG ATA AGT GCC AGC CGA GCT-3′; RV1: 5′- *Xba*I CAT AAC TGC CAC GCA GGA-3′; FW2: 5′-*Xba*I AGC TGC CAT TCA GGG AGG T-3′; RV2: 5′-*Hin*dIII TTA GAG GTC TTC TTC TGA GAT GAG CTT CTG CTC CTG TTT TTC CTC CTT TTG ATC TTC C-3′), and ΔCT 1–434 (FW: 5′-*Bam*HI ATG ATA AGT GCC AGC CGA GCT-3′; RV: *Hin*dIII TTA GAG GTC TTC TTC

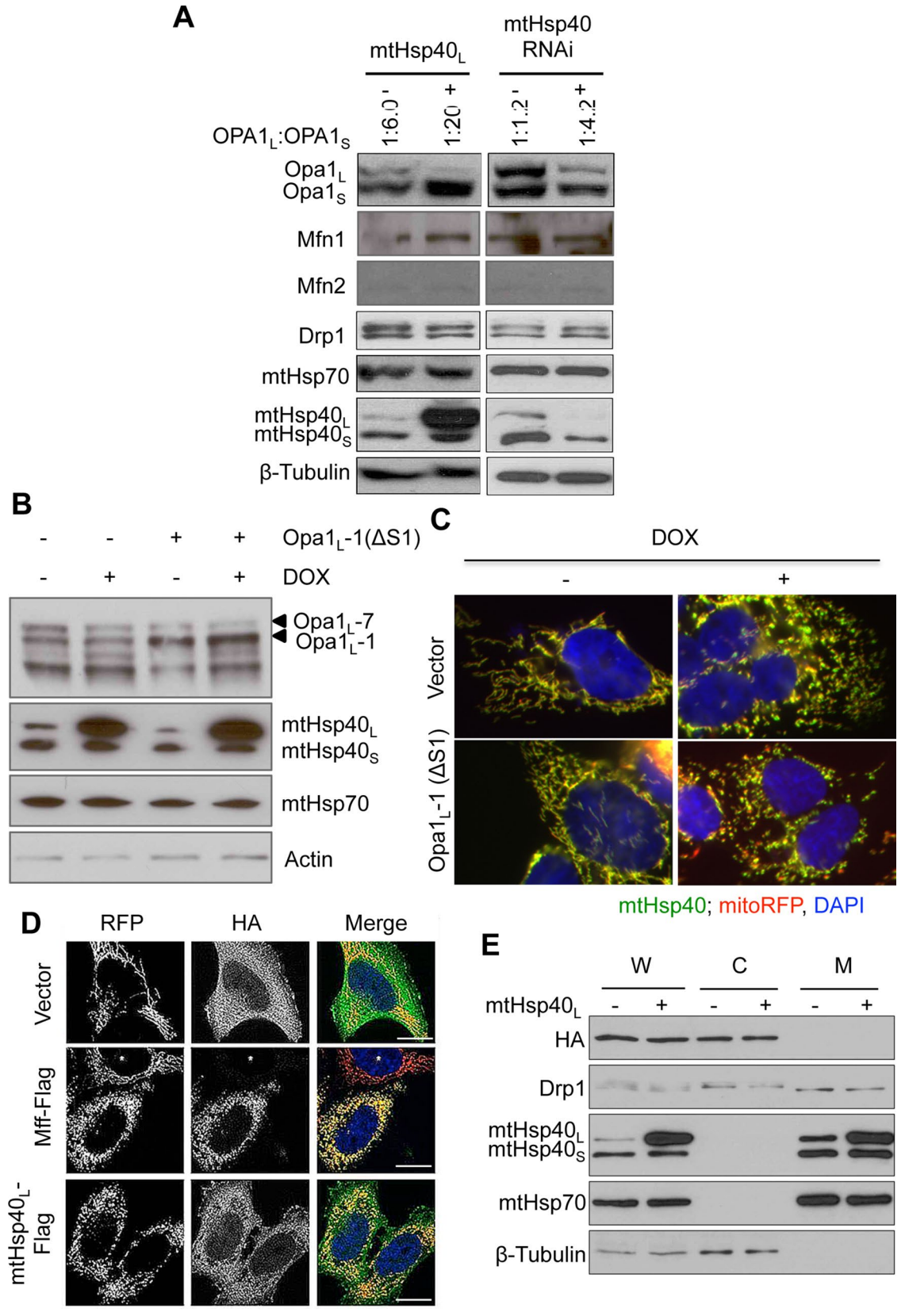

FIGURE 6: Deregulation of mtHsp40 promotes Opa1$_L$ cleavage. (A) Opa1$_S$ accumulation upon mtHsp40 deregulation. Left, lysates from HeLa-mitoRFP cells transfected with GFP or mtHsp40$_L$ analyzed by Western blotting for Opa1, Mfn1, Mfn2, and Drp1. Right, lysates from HeLa-mitoRFP transfected with scramble siRNA or mtHsp40 siRNA. The Opa1$_L$:Opa1$_S$ ratio was calculated with densities of Opa1$_L$ and Opa1$_S$ bands using ImageJ software (National Institutes of Health, Bethesda, MD). (B) Specific promotion of Opa1$_L$-7 cleavage (ΔS1) in the presence of mtHsp40 deregulation.

TGA GAT GAG CTT CTG CTC ATC CGT GAC ATC GCC GGC CAA-3′).

Cell culture, transfection, and stable clones

HeLa-mtRFP cells were cultured as described (Cereghetti *et al.*, 2008). Cells were transfected using Lipofectamine 2000 Reagent (Life Technologies, Burlington, Canada) for plasmids and HiPerfect Transfection Reagent (Qiagen) for siRNAs following manufacturers' instructions. HEK293-mitoRFP-mtHsp40$_L$ stable clones were generated by repeated dilution of HEK293-TetR cells (provided by Ebba Kurz, University of Calgary, Calgary, Canada) every 2 d after cotransfection with pRS-mitoRFP and pcDNA4/TO-mtHsp40$_L$ and antibiotic selection (2 µg/ml puromycin and 100 µg/ml blasticidin) of expressing cells.

Imaging, image analysis, and biochemistry

For immunofluorescence, cells grown on 22-mm glass coverslips were fixed in 4% (wt/vol) paraformaldehyde in phosphate-buffered saline (PBS; 30 min, 4°C), permeabilized with 3% bovine serum albumin and 0.2% Triton X-100, and incubated with primary anti-HA (rat, 1:100; home made) or anti-Flag (mouse, 1:100; Sigma-Aldrich, Oakville, Canada) antibodies. Cells were then stained with fluorescent secondary anti-rat immunoglobulin G (IgG)–Alexa Fluor 488 (1:1000; Invitrogen, Burlington, Canada) or anti-mouse IgG–Alexa Fluor 488 (1:1000) antibodies. For fluorescence microscopy, red (for mtRFP) and green (for HA or Flag) images were acquired simultaneously using 63×/1.40 oil/differential interference contrast objective and two separate 568- and 488 nm excitations on the detector assembly of an Axiovert fluorescence microscope with Apoptome (Carl Zeiss, Vancouver, Canada). Images were background corrected, acquired, and stored for analysis using AxioVision software (Carl Zeiss). Cells showing mixed and unclear morphologies of mitochondria were not counted. Mitochondrial fractionation was performed using the QProteome Mitochondria Isolation Kit (Qiagen) according to the manufacturer's instructions. For immunoblotting, proteins were separated by 8, 10, or 12% Tris-glycine SDS–PAGE and transferred onto nitrocellulose or polyvinylidene fluoride membranes (Bio-Rad, Mississauga, Canada). Membranes were incubated with the following primary antibodies: anti-mtHsp40$_{L/S}$ (mouse, 1:1000; Santa Cruz Biotechnology, Dallas, TX), anti–β-tubulin (rabbit, 1:5000; Santa Cruz Biotechnology), anti-Drp1 (mouse, 1:1000; BD Biosciences, Mississauga, Canada), anti-Opa1 (mouse, 1:1000; BD Biosciences), anti-HA (rat, 1:2000; home made), anti-Flag (mouse or rabbit, 1:1000; Sigma-Aldrich), anti-Myc (mouse, 1:2000; Invitrogen), anti-Mfn1 (chicken, 1:500; gift of David Chan, California Institute of Technology, Pasadena, CA), anti-Mfn2 (mouse, 1:250; gift of David Chan), and anti-mtHsp70 (mouse, 1:5000; Thermo Scientific, Burlington, Canada). Isotype-matched secondary antibodies conjugated to horseradish peroxidase were incubated at 1:5000, and bands were detected using enhanced chemiluminescence substrate (Pierce Biotechnology, Burlington, Canada).

Transmission electron microscopy

Cells were fixed for 1 h at 4°C using 2.5% (vol/vol) glutaraldehyde (Sigma-Aldrich). Thin sections were imaged on a Hitachi (Toronto, Canada) H-7650 transmission electron microscope at the Microscopy and Imaging Facility, University of Calgary.

ATP assay

Cells were trypsinized, and >10^5 cells were subjected to ATP assays using the ATP bioluminescence assay kit (Sigma-Aldrich) according to the manufacturer's instructions.

OCR analysis

OCR was measured using the Seahorse XF24 Extracellular Flux Analyzer (Seahorse Bioscience, Billerica, MA) according to the manufacturer's instructions. Briefly, 40,000 cells/well grown on XF24 cell culture microplates were switched to assay medium (unbuffered DMEM supplemented with 10 mM sodium pyruvate and 10 mM glucose) and incubated without CO_2 at 37°C for 1 h. Next the mitochondrial function assay was performed with sequential injection of oligomycin (1 µg/ml; Enzo, Life Sciences, Brockville, Canada), carbonyl cyanide-4-(trifluoromethoxy)phenylhydrazone (0.5 µM; Sigma-Aldrich), and rotenone (1 µM; Enzo) at the indicated time intervals.

mtDNA quantification and mitochondria quantity measurement

Total DNA was isolated from 10^6 cells using the QIAamp DNA Mini Kit (Qiagen) according to the manufacturer's instructions and quantified by using Nanovue Plus (GE Healthcare, Mississauga, Canada). The mitochondrial DNA amount relative to genomic DNA content was analyzed by using an ABI StepOnePlus Real-Time PCR system (Applied Biosystems, Burlington, Canada). Primers were designed for mitochondrial COX-I (FW: 5′-ACC CTA GAC CAA ACC TAC GCC AAA-3′; RV: 5′-TAG GCC GAG AAA GTG TTG TGG GAA-3′) and nuclear 16S rRNA (FW: 5′-GTA ACC CGT TGA ACC CCA TT-3′; RV: 5′-CCA TCC AAT CGG TAG TAG CG-3′). For mitochondrial content analysis, cells grown on six-well tissue culture plates were stained by MitoTracker Green (100 µM; Life Technologies) in Hank's balanced salt solution (HBSS) solution for 30 min. Cells were trypsinized, collected, and resuspended in HBSS. Green fluorescence intensity was analyzed by flow cytometry (LSR II; BD Biosciences).

HEK293-mitoRFP-mtHsp40$_L$ cells transfected with control or Opa1$_L$-1 (ΔS1) (10 ng/ml, 24 h) were treated with PBS or DOX (10 ng/ml, 24 h). Cell lysates were analyzed by Western blotting. (C) Effects of expression of Opa1$_L$-1 (ΔS1) on mitochondrial morphology. Cells as described in B were immunostained using mtHsp40 antibodies (green), and mitochondria were visualized with RFP (red). Representative images. Insets, magnified images of boxed regions. Scale bars, 10 µm. (D) Drp1 localization in cells overexpressing mtHsp40. HeLa-mitoRFP cells were cotransfected with HA-Drp1 and the indicated plasmids and analyzed for expression of Mff-FLAG and mtHsp40-FLAG (anti-FLAG) and Drp1 localization (anti-HA). Mitochondrial morphologies were visualized with RFP. Scale bars, 10 µm. Asterisk indicates untransfected cells. (E) Drp1 retention in the cytosol of cells overexpressing mtHsp40$_L$. Cytosol and crude mitochondrial fractions were prepared from the indicated cells and analyzed by Western blotting for HA and Drp1, mtHsp70 (mitochondrial), and β-tubulin (cytosolic). C, cytosolic fraction; M, mitochondrial fraction; W, whole-cell extract.

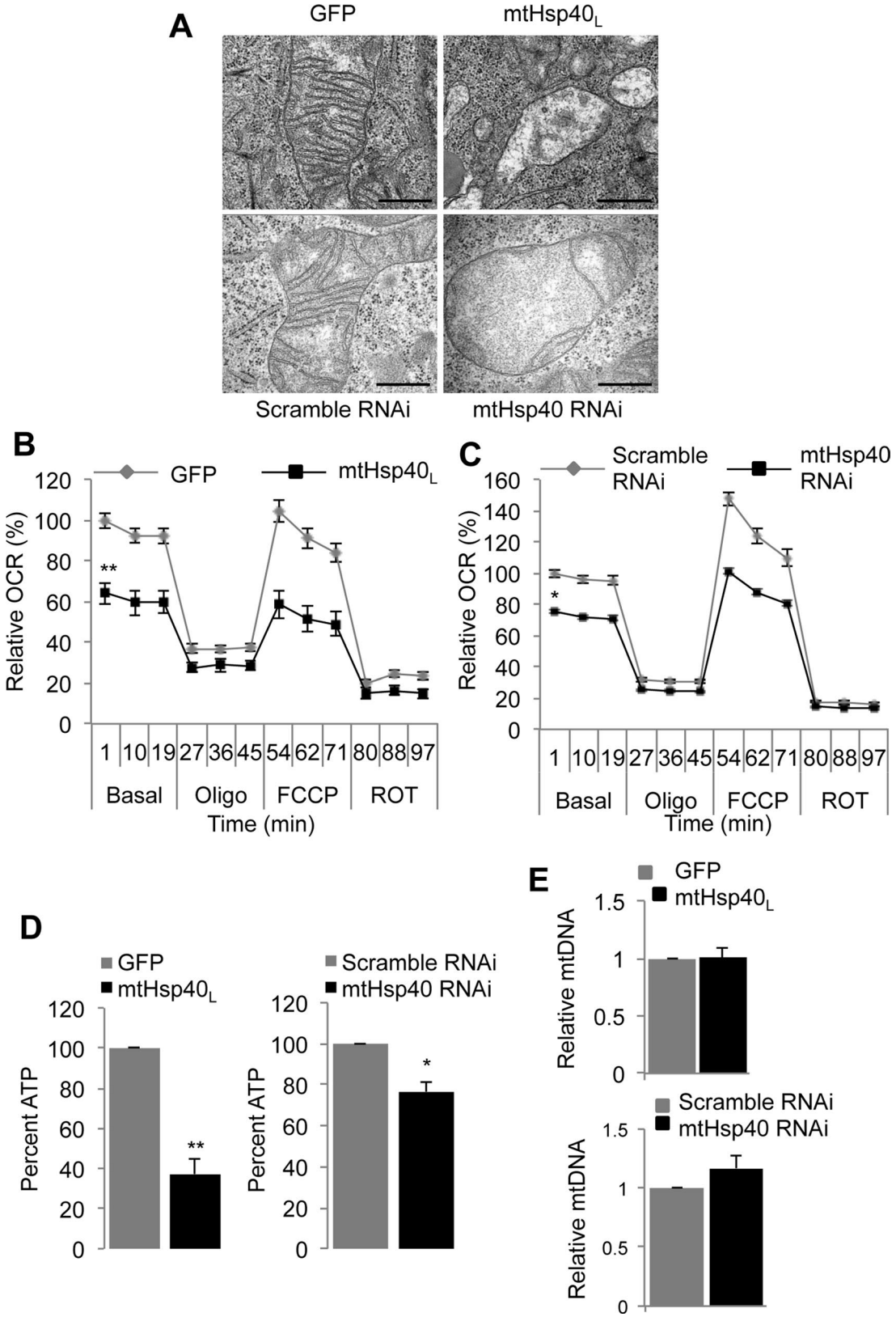

FIGURE 7: Fragmented mitochondria become defective in cristae development and OXPHOS. (A) Representative TEM fields of mitochondria in HeLa-mitoRFP cells expressing mtHsp40$_L$ and mtHsp40 siRNA. Scale bars, 500 nm. Reduction in OCR (B, C) and ATP levels (D) in fragmented mitochondria. Quantitation of ATP and OCR level was done from cells expressing mtHsp40$_L$ and mtHsp40 siRNA by plotting the percentage of control. Data were obtained from three independent experiments. Error bars, SEM; $^{**}p < 0.01$, $^{*}p < 0.05$. Unaffected mitochondrial DNA amount in fragmented mitochondria. Quantitation of mtDNA (E) was done from cells expressing mtHsp40$_L$ and mtHsp40 siRNA by plotting the relative amount against control. Data were obtained from three independent experiments. Error bars, SEM.

ACKNOWLEDGMENTS

We thank D. Chan and A. M. van der Bliek for providing antibodies and vectors, as well as for discussions, and S. Grewal for providing critical feedback. This work was supported in part by grants from the Alberta Cancer Research Institute (23123), the Canada Research Chairs Program (950-203751), and the Canadian Institutes of Health Research (MOP97962) to S.W.K. and from the Alberta Children's Hospital Research Institute (J.M.R.).

REFERENCES

Ahn BY, Trinh DLN, Zajchowski LD, Lee B, Elwi AN, Kim S-W (2010). Tid1 is a new regulator of p53 mitochondrial translocation and apoptosis in cancer. Oncogene 29, 1155–1166.

Anand R, Wai T, Baker MJ, Kladt N, Schauss AC, Rugarli E, Langer T (2014). The i-AAA protease YME1L and OMA1 cleave OPA1 to balance mitochondrial fusion and fission. J Cell Biol 204, 919–929.

Burbulla LF, Schelling C, Kato H, Rapaport D, Woitalla D, Schiesling C, Schulte C, Sharma M, Illig T, Bauer P (2010). Dissecting the role of the mitochondrial chaperone mortalin in Parkinson's disease: functional impact of disease-related variants on mitochondrial homeostasis. Hum Mol Genet 19, 4437–4452.

Cereghetti GM, Stangherlin A, Martins de BO, Chang CR, Blackstone C, Bernardi P, Scorrano L (2008). Dephosphorylation by calcineurin regulates translocation of Drp1 to mitochondria. Proc Natl Acad Sci USA 105, 15803–15808.

Chen H, Detmer SA, Ewald AJ, Griffin EE, Fraser SE, Chan DC (2003). Mitofusins Mfn1 and Mfn2 coordinately regulate mitochondrial fusion and are essential for embryonic development. J Cell Biol 160, 189–200.

Cipolat S, Martins de BO, Dal ZB, Scorrano L (2004). OPA1 requires mitofusin 1 to promote mitochondrial fusion. Proc Natl Acad Sci USA 101, 15927–15932.

Cogliati S, Frezza C, Soriano ME, Varanita T, Quintana-Cabrera R, Corrado M, Cipolat S, Costa V, Casarin A, Gomes LC, *et al*. (2013). Mitochondrial cristae shape determines respiratory chain supercomplexes assembly and respiratory efficiency. Cell 155, 160–171.

Collins TJ, Berridge MJ, Lipp P, Bootman MD (2002). Mitochondria are morphologically and functionally heterogeneous within cells. EMBO J 21, 1616–1627.

Ehses S, Raschke I, Mancuso G, Bernacchia A, Geimer S, Tondera D, Martinou JC, Westermann B, Rugarli EI, Langer T (2009). Regulation of OPA1 processing and mitochondrial fusion by m-AAA protease isoenzymes and OMA1. J Cell Biol 187, 1023–1036.

Frezza C, Cipolat S, Martins de BO, Micaroni M, Beznoussenko GV, Rudka T, Bartoli D, Polishuck RS, Danial NN, De SB (2006). OPA1 controls apoptotic cristae remodeling independently from mitochondrial fusion. Cell 126, 177–189.

Gegg ME, Cooper JM, Chau KY, Rojo M, Schapira AH, Taanman JW (2010). Mitofusin 1 and mitofusin 2 are ubiquitinated in a PINK1/parkin-dependentmanner upon induction of mitophagy. Hum Mol Genet 19, 4861–4870.

Gomes LC, Di BG, Scorrano L (2011). During autophagy mitochondria elongate, are spared from degradation and sustain cell viability. Nat Cell Biol 13, 589–598.

Guillery O, Malka F, Landes T, Guillou E, Blackstone C, Lombes A, Belenguer P, Arnoult D, Rojo M (2008). Metalloprotease-mediated OPA1 processing is modulated by the mitochondrial membrane potential. Biol Cell 100, 315–325.

Hageman J, van Waarde MA, Zylicz A, Walerych D, Kampinga HH (2011). The diverse members of the mammalian HSP70 machine show distinct chaperone-like activities. Biochem J 435, 127–142.

Hartl FU, Bracher A, Hayer-Hartl M (2011). Molecular chaperones in protein folding and proteostasis. Nature 475, 324–332.

Head B, Griparic L, Amiri M, Gandre-Babbe S, van der Bliek AM (2009). Inducible proteolytic inactivation of OPA1 mediated by the OMA1 protease in mammalian cells. J Cell Biol 187, 959–966.

Iosefson O, Sharon S, Goloubinoff P, Azem A (2012). Reactivation of protein aggregates by mortalin and Tid1—the human mitochondrial Hsp70 chaperone system. Cell Stress Chaperones 17, 57–66.

Jendrach M, Mai S, Pohl S, Voth M, Bereiter-Hahn J (2008). Short- and long-term alterations of mitochondrial morphology, dynamics and mtDNA after transient oxidative stress. Mitochondrion 8, 293–304.

Kampinga HH, Craig EA (2010). The HSP70 chaperone machinery: J proteins as drivers of functional specificity. Nat Rev Mol Cell Biol 11, 579–592.

Kim SW, Chao TH, Xiang R, Lo JF, Campbell MJ, Fearns C, Lee JD (2004). Tid1, the human homologue of a Drosophila tumor suppressor, reduces the malignant activity of ErbB-2 in carcinoma cells. Cancer Res 64, 7732–7739.

Lee B, Elwi AN, Meijnderta HC, Braun JEA, Kim S-W (2012). Mitochondrial chaperone DnaJA3 induces Drp1-dependent mitochondrial fragmentation. Int J Biochem Mol Biol 44, 1366–1376.

Legros F, Lombes A, Frachon P, Rojo M (2002). Mitochondrial fusion in human cells is efficient, requires the inner membrane potential, and is mediated by mitofusins. Mol Biol Cell 13, 4343–4354.

Loson OC, Song Z, Chen H, Chan DC (2013). Fis1, Mff, MiD49, and MiD51 mediate Drp1 recruitment in mitochondrial fission. Mol Biol Cell 24, 659–667.

Norton M, Ng ACH, Baird S, Dumoulin A, Shutt T, Mah N, Andrade-Navarro MA, McBride HM, Screaton RB (2014). ROMO1 is an essential redox-dependent regulator of mitochondrial dynamics. Sci Signal 7, ra10.

Otera H, Wang C, Cleland MM, Setoguchi K, Yokota S, Youle RJ, Mihara K (2010). Mff is an essential factor for mitochondrial recruitment of Drp1 during mitochondrial fission in mammalian cells. J Cell Biol 191, 1141–1158.

Pellegrino MW, Nargund AM, Kirienko NV, Gillis R, Fiorese CJ, Haynes CM (2014). Mitochondrial UPR-regulated innate immunity provides resistance to pathogen infection. Nature 516, 414–417.

Schmidt O, Pfanner N, Meisinger C (2010). Mitochondrial protein import: from proteomics to functional mechanisms. Nat Rev Mol Cell Biol 11, 655–667.

Song Z, Chen H, Fiket M, Alexander C, Chan DC (2007). OPA1 processing controls mitochondrial fusion and is regulated by mRNA splicing, membrane potential, and Yme1L. J Cell Biol 178, 749–755.

Suen DF, Norris KL, Youle RJ (2008). Mitochondrial dynamics and apoptosis. Genes Dev 22, 1577–1590.

Yoon Y, Krueger EW, Oswald BJ, McNiven MA (2003). The mitochondrial protein hFis1 regulates mitochondrial fission in mammalian cells through an interaction with the dynamin-like protein DLP1. Mol Cell Biol 23, 5409–5420.

Zhao J, Liu T, Jin S, Wang X, Qu M, Uhlen P, Tomilin N, Shupliakov O, Lendahl U, Nister M (2011). Human MIEF1 recruits Drp1 to mitochondrial outer membranes and promotes mitochondrial fusion rather than fission. EMBO J 30, 2762–2778.